Fuzzy Adaptive Vibration Suppression And Noise Filtering for Flexible Robot Control

Anthony Green and Jurek Z. Sasiadek, *Senior Member, IEEE*

Abstract— **Tracking the end effector of a two-link flexible robot is simulated using control strategies with an inverse dynamics robot model and Jacobian transpose control law. Results are presented for linear quadratic Gaussian (LQG) dynamic regulator with extended Kalman filter (EKF); LQG with fuzzy logic adaptive EKF (FLAEKF); LQG with EKF and FLAEKF combined with fuzzy logic system (FLS) vibration suppression. In general, FLS vibration suppression overrides noise filtering in achieving tracking accuracy. In comparison with classical PID control or even with more advanced adaptive control strategies FLS vibration suppression gives better trajectory tracking while execution time remains acceptable.**

I. Introduction

OPERATIONAL problems with space robots relate to several factors, one most importantly being structural flexibility and subsequently significant difficulties with position control. Elastic vibrations of the links coupled with their large rotation and nonlinear dynamics is the primary cause. This paper demonstrates the control of a two-link flexible robot end effector mounted on a stationary spacecraft tracking a square trajectory 12.6m x 12.6m. The dominant assumed mode of vibration for an Euler-Bernoulli cantilever beam is coupled with rigid-link dynamics to form an Euler-Lagrange inverse flexible dynamics robot model. Initially, tracking results are obtained without vibration suppression or noise filtering. Then, EKF and FLAEKF state estimators are implemented in a linear quadratic Gaussian (LQG) dynamic regulator to determine their effects on tracking accuracy when the robot system is subjected to process and measurement noise. Finally, a fuzzy logic system (FLS) is included to adapt the control law and suppress residual vibrations. Square trajectory tracking studies for rigid and flexible dynamics models were presented in previous work. Good results were achieved using an input shaping method to reduce residual vibrations coupled with an inverse kinematics control strategy for both linear and nonlinear control laws and a recursive order-n algorithm to model a two-link flexible robot [1]. A FLS adaptive control strategy is used to suppress vibrations in tracking a flexible robot without noise filtering [2]. Results are compared in tracking a two-link robot manipulator for control with linear quadratic regulator (LQR) and LQG with Kalman filter, EKF and FLAEKF [3]. A model reference adaptive control (MRAC) technique using a modal expansion for the first three significant vibration modes is used to control a single-link flexible robot resulting in reduced errors and decreased settling time of transient responses to step inputs [4].

A. Green is a PhD candidate in the Mechanical and Aerospace Engineering Department, Carleton University, Ottawa, Ontario, K1S 5B6, Canada (phone: 416 239 4019, e-mail: agreen2@connect.carleton.ca).

J. Z. Sasiadek is with the Mechanical and Aerospace Engineering Department, Carleton University, Ottawa, ON K1S 5B6, Canada (phone : 631 520 2600, e-mail: jsas@ccs.carleton.ca).

II. Flexible Robot

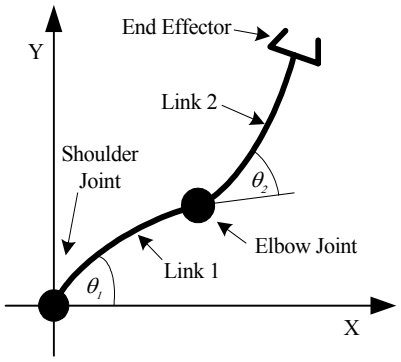

Fig. 1. Flexible robot.

The flexible robot shown in Fig. 1 has planar motion and vibration modes. Gravity and friction effects are omitted. Robot parameters are; length of each link $L_1 = L_2 = 4.5$m; flexural rigidity EI = 1676 N-m^2 and link mass density ρ = 0.335 kg/m [1].

A. Rigid Dynamics

The nonlinear rigid-link dynamics of a multilink robot is derived by the Euler-Lagrange formulation in terms of kinetic and potential energies. Given an independent set of generalized coordinates, $q_i = q_1,.....,q_n$, the total kinetic and potential energies stored in the system, T and U respectively, is defined by the Lagrangian [5].

$$\mathfrak{L}\left(q_i, \dot{q}_i\right) = T - U, \qquad i = 1,.....,n \quad (1)$$

For a robot subjected to generalized force F_i acting on a generalized coordinate q_i the dynamic equations of motion

are given by.

$$\frac{d}{dt}\frac{\partial \mathfrak{L}}{\partial \dot{q}_i} - \frac{\partial \mathfrak{L}}{\partial q_i} = F_i, \qquad i = 1,.....,n \tag{2}$$

Kinetic energy is given by.

$$T = \frac{1}{2}\sum_{i=1}^{n}\sum_{j=1}^{n} M_{ij}\dot{q}_i\dot{q}_j, \tag{3}$$

For space robot applications the gravity potential energy is zero and omitted in this presentation. For an n-degree-of-freedom (n-dof) robot the Euler-Lagrange rigid dynamics equations are [5].

$$\boldsymbol{\tau} = \mathbf{M}(\theta)\ddot{\theta} + \mathbf{C}(\dot{\theta},\theta)\dot{\theta} \tag{4}$$

B. Flexible Dynamics

Accurate tracking control of a flexible robot is compounded by deformation of its flexible links and an effective control strategy must be able to suppress residual vibrations to achieve tracking accuracy. Coupling assumed modes of vibration for an Euler-Bernoulli beam with rotating rigid links models the two-link flexible robot and captures its nonlinear flexible multibody interactions. The flexible dynamics equations are derived in Euler-Lagrange form. Assumed modes accommodate configuration changes during operation, whereas, natural modes must be continually recomputed [6]. For an Euler-Bernoulli beam with flexural rigidity EI and uniformly distributed load p(x,t), the equation of motion is given by.

$$\partial^2/\partial x^2\left(EI\,\partial^2 u(x,t)/\partial x^2\right)dx + m(x)\,\partial^2 u(x,t)/\partial t^2 = p(x,t) \tag{5}$$

The normal modes $\phi_i(x)$ must satisfy (6).

$$\left[EI\phi_i''(x)\right]'' - \omega_i^2 m(x)\phi_i(x) = 0 \tag{6}$$

and its boundary conditions

$$\phi_i(0) = \phi_i'(0) = 0; \quad \phi_i''(L) = \phi_i'''(L) = 0$$

Substituting assumed modes for normal modes leads to an approximate solution for (5) as the deformation of a beam subjected to transverse vibrations given by [7].

$$u(x,t) = \sum_{i=1}^{n}\phi_i(x)q_i(t) \tag{7}$$

where; $\phi_i(x)$ are assumed mode shapes.

C. Cantilever Assumed Modes

From transverse beam vibration theory, cantilever mode shapes are given by [7].

$$\phi_{ci}(x) = A\left[\cosh\lambda_{ci}x - \cos\lambda_{ci}x - k_{ci}(\sinh\lambda_{ci}x - \sin\lambda_{ci}x)\right] \tag{8}$$

where; $A = 0.1$ is an arbitrary constant, $\lambda_{ci}L = (i - 0.5)\pi$, $i = 1,\ldots\ldots,n$ are numerically approximated roots of the characteristic equation $\cos(\lambda_{ci}L)\cosh(\lambda_{ci}L) + 1 = 0$ and $k_{ci} = \cos\lambda_{ci}L + \cosh\lambda_{ci}L / \sin\lambda_{ci}L + \sinh\lambda_{ci}L$.

Modal frequencies are given by.

$$\omega_{ci} = (\lambda_{ci}L)^2\sqrt{EI/\rho L^4} \tag{9}$$

The deformation $u(x,t)$ in (7) substitutes into the Euler-Lagrange dynamics equations for which elastic kinetic and potential energies are given by [7].

$$T_e = 1/2\left(\sum_i^n\sum_j^n \dot{q}_i\dot{q}_j\int_0^L \phi_i\phi_j m(x)dx\right) \tag{10}$$

$$U_e = 1/2\left(\sum_i^n\sum_j^n \dot{q}_i\dot{q}_j\int_0^L EI\phi_i''\phi_j''dx\right) \tag{11}$$

Combining rigid and elastic terms the matrix equations are given by [8].

$$\boldsymbol{\tau} = \mathbf{M}(\mathbf{q})\ddot{\mathbf{q}} + \mathbf{C}(\dot{\mathbf{q}},\mathbf{q})\dot{\mathbf{q}} + \mathbf{K}\mathbf{q} \tag{12}$$

M contains rigid and flexible link elements, **C** contains rigid and elastic Coriolis and centrifugal effects and **K** is a stiffness matrix. The generalized coordinate vector **q** contains joint angles and flexible link deformations. The calculation of assumed modes assumes small elastic deformation where second-order terms of interacting elastic modes can be neglected and orthogonality simplifies (12). Omitting elastic Coriolis and centrifugal components gives the rigid dynamics coupling matrix **C** in (4). A complete derivation of full dynamics equations for a multi-degree-of-freedom (multi-dof) manipulator was previously published [9].

The Jacobian transpose reference control law is given by [2].

$$\boldsymbol{\tau}_r = \mathbf{J}^T(\theta)\left[\mathbf{K}_p\begin{pmatrix}e_x\\e_y\end{pmatrix} + \mathbf{K}_d\begin{pmatrix}\dot{e}_x\\\dot{e}_y\end{pmatrix}\right] \tag{13}$$

Proportional and derivative (PD) gains for the dominant assumed mode are given by.

$$\mathbf{K_p} = \mathrm{diag}\left[\omega_{c1}^2 \quad \omega_{c1}^2\right] = \mathrm{diag}\left[150.79 \quad 150.79\right] \tag{14}$$

$$\mathbf{K_d} = \mathrm{diag}\left[2\zeta\omega_{c1} \quad 2\zeta\omega_{c1}\right] = \mathrm{diag}\left[17.364 \quad 17.364\right] \tag{15}$$

for $\omega_{c1} = 12.28$ Hz and damping ratio $\zeta. = 0.707$.

Rigid-link robot kinematic equations relating end effector positions x, y to joint angles θ_1, θ_2 shown in Fig. 1 are given by [5].

$$x = L_1\cos(\theta_1) + L_2\cos(\theta_1 + \theta_2) \tag{16}$$

$$y = L_1\sin(\theta_1) + L_2\sin(\theta_1 + \theta_2) \tag{17}$$

Using (16) and (17) the Jacobian J is derived as [5].

$$\mathbf{J} = \begin{bmatrix} \frac{\partial x}{\partial \theta_1} & \frac{\partial x}{\partial \theta_2} \\ \frac{\partial y}{\partial \theta_1} & \frac{\partial y}{\partial \theta_2} \end{bmatrix} \tag{18}$$

$$= \begin{bmatrix} -L_1 \sin\theta_1 - L_2 \sin(\theta_1 + \theta_2) & -L_2 \sin(\theta_1 + \theta_2) \\ L_1 \sin\theta_1 + L_2 \cos(\theta_1 + \theta_2) & L_2 \cos(\theta_1 + \theta_2) \end{bmatrix}$$

III. Control Strategies

The control strategy shown in Fig. 5 may comprise a combination of different techniques including; an EKF or FLAEKF for noise filtering, with or without FLS vibration suppression. Because of the difficulty with deriving and modeling nonminimum phase (zero dynamics) state estimators, the filters used in this study are those derived for a minimum phase rigid-link dynamics robot manipulator [3]. The control law is transpose Jacobian with PD feedback and may be adapted by a FLS to achieve vibration suppression. The EKF and FLAEKF are shown in Figs. 6 and 7. These filters are implemented as part of a linear quadratic Gaussian (LQG) dynamic regulator that includes separate linear quadratic regulator (LQR) full state feedback gains and extended Kalman filter recursive subroutines [3], [10]. The FLAEKF provides a more accurate state estimate for control law regulation and elimination of tracking divergence experienced with an EKF [3].

A. . Extended Kalman Filter

The EKF recursive subroutine shown in Fig. 6 is based upon discrete linearized state-space equations for a rigid dynamics robot given by [3], [10], [11], [12].

$$\mathbf{x}_{k+1} = \mathbf{\Phi}_k \mathbf{x}_k + \mathbf{w}_k \tag{19}$$

$$\mathbf{z}_k = \mathbf{C}_k \mathbf{x}_k + \mathbf{v}_k \tag{20}$$

for time increments $k \geq 0$ where; z_k is a measurement vector; $\mathbf{\Phi}_k$ is a state transition matrix; $\mathbf{w}_k \sim N(\mu, \mathbf{Q}_k)$ and $\mathbf{v}_k \sim N(\mu, \mathbf{R}_k)$ are process and measurement noise; $\mathbf{Q}_k = E[\mathbf{w}_k \mathbf{w}_k^T]$, $\mathbf{R}_k = E[\mathbf{v}_k \mathbf{v}_k^T]$ and $\mathbf{N}_k = E[\mathbf{w}_k \mathbf{v}_k^T]$ are process noise, measurement noise covariance and cross-covariance matrices respectively.

EKF state estimation is a well-established theory based on *a priori* and *a posteriori* state estimates; *a priori* and *a posteriori* error covariance matrices; projected state estimate and error covariance matrices and Kalman gain. It is left to the reader to review extensive literature on this topic [10], [11], [12], [13].

B. Fuzzy Logic Adaptive Extended Kalman Filter

The FLAEKF shown in Fig. 7 is an extension to the EKF in which the recursive equations are adapted by a weighting parameter α. Adaptive noise covariance, cross-covariance and error covariance matrices are given by the following equations [3], [13].

$$\mathbf{Q}_\alpha = \mathbf{Q}_k \alpha^{-2(k+1)} \tag{21}$$

$$\mathbf{R}_\alpha = \mathbf{R}_k \alpha^{-2(k+1)} \tag{22}$$

$$\mathbf{N}_\alpha = \mathbf{N}_k \alpha^{-2(k+1)} \tag{23}$$

$$\mathbf{P}_k^{\alpha-} = \mathbf{P}_k^- \alpha^{2k}, \ \alpha \geq 1 \tag{24}$$

As *k* increases, $\mathbf{Q}_k$ and $\mathbf{R}_k$ decrease so the most recent measurement is weighted higher. The FLAEKF adapts the value of α according to the magnitude of $\mathbf{P}_k$ and non-zero means $\hat{\bar{\mathbf{x}}}$ such that optimality and a zero-mean white noise condition is maintained. The FLAEKF behaves as an EKF when $\alpha = 1$. Using the Kalman gain equation for an EKF and (21)-(24), the Kalman gain K_k for the FLAEKF is derived as [3], [13].

$$\mathbf{K}_k = \left(\alpha^2 \mathbf{P}_k^{\alpha-} + \mathbf{N}_k\right) \begin{pmatrix} \alpha^2 \mathbf{C}_k \mathbf{P}_k^{\alpha-} \mathbf{C}_k^T \\ + \mathbf{R}_k + \mathbf{C}_k \mathbf{N}_k \\ + \mathbf{N}_k^T \mathbf{C}_k^T \end{pmatrix}^{-1} \tag{25}$$

The *a priori* state estimate is given as.

$$\hat{\mathbf{x}}_k^- = \mathbf{\Phi}_k \hat{\mathbf{x}}_k \tag{26}$$

and error covariance matrix is given as.

$$\mathbf{P}_{k+1}^{\alpha-} = \alpha^2 \mathbf{\Phi}_k \mathbf{P}_k^{\alpha-} \mathbf{\Phi}_k^T + \mathbf{Q}_k \tag{27}$$

The *a posteriori* state estimate is given as.

$$\hat{\mathbf{x}}_k = \hat{\mathbf{x}}_k^- + \mathbf{K}_k \left(\mathbf{z}_k - \hat{\mathbf{z}}_k^-\right) \tag{28}$$

where; $\hat{\mathbf{z}}_k^-$ is a predictive measurement vector and $\mathbf{z}_k - \hat{\mathbf{z}}_k^-$ a measurement residual vector. The *a priori* state estimates and error covariance at time $k = 0$ are $\hat{\mathbf{x}}_0^-$ and $\mathbf{P}_0^{\alpha-}$.

The *a posteriori* error covariance matrix is given as.

$$\mathbf{P}_k^\alpha = \left(\mathbf{I} - \mathbf{K}_k \mathbf{C}_k\right) \mathbf{P}_k^{\alpha-} - \mathbf{K}_k \frac{\mathbf{N}_k^T}{\alpha^2} \tag{29}$$

for initial condition at $k = 0$, $\mathbf{P}_0^{\alpha-} = \mathbf{P}_0$

Assuming Gaussian statistics and from a *conditional density viewpoint* the mean-square estimation error is given as [12].

$$\hat{\mathbf{x}}_k = E\left(\mathbf{x}_k | \mathbf{z}_k^*\right) \tag{30}$$

The mean state estimate is given as.

$$\hat{\bar{\mathbf{x}}}_k = \hat{\mathbf{x}}_k^- + \mathbf{M}_k \left(\mathbf{z}_k - \hat{\mathbf{z}}_k^-\right) \tag{31}$$

where;

$$\mathbf{M} = \mathbf{P}_k^- \mathbf{C}_k^T \left(\mathbf{C}_k \mathbf{P}_k^- \mathbf{C}_k^T + \mathbf{R}_k\right)^{-1} \tag{32}$$

and the error covariance of the residuals is given as.

$$\mathbf{P}_z = \left[\left(\mathbf{P}_k^-\right)^{-1} + \mathbf{C}_k^T \mathbf{R}_k^{-1} \mathbf{C}_k\right]^{-1} \tag{33}$$

The fuzzy variables each have four triangular membership functions and all universes of discourse fall into the positive right half-plane to satisfy the condition

$\alpha \geq 1$ [14]. Input variables are mean and error covariance of the residuals given by (31) and (33). Verbal descriptors for zero (ZERO), small (S), medium (M), and large (L) are used to label membership functions shown in Figs. 2 (a), (b) and (c) that generate sixteen fuzzy rules of the form;

IF P_z is S AND Mean is S THEN α is M

The fuzzy rules form the rule matrix given in Table I.

Process and measurement white noise input the system as Gaussian random number distributions whose variance are noise covariance $\mathbf{Q}_k$ and $\mathbf{R}_k$ in the EKF recursive equations. The cross covariance $\mathbf{N}_k = E[\mathbf{w}_k \mathbf{v}_k^T]$ models the noise cross-correlation of control inputs and observed measurement outputs and is computed as the product of standard deviations of $\mathbf{Q}_k$ and $\mathbf{R}_k$ diagonal elements, such that;

$\mathbf{N}_k = E[\mathbf{w}_k \mathbf{v}_k^T] \sim \sigma_w \sigma_v$, where; $\mathbf{N}_k = 1$ for $\mathbf{w}_k = \mathbf{v}_k = N(0, 1)$.

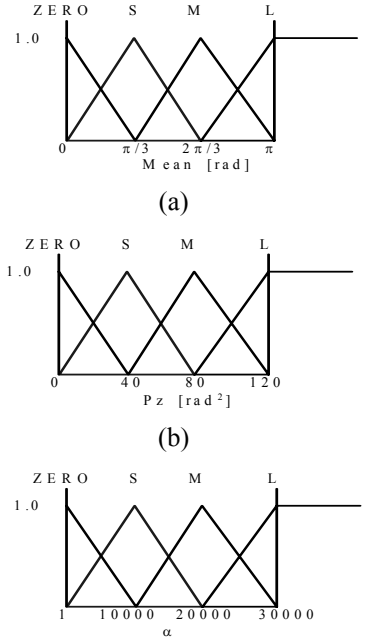

Fig. 2. Fuzzy membership functions: (a) Mean, (b) Pz , (c) α.

TABLE I
FLAEKF RULE MATRIX

		Mean			
	α	Z	S	M	L
Pz	Z	Z	S	M	L
	S	S	M	L	L
	M	M	L	L	L
	L	L	L	L	L

For either an EKF or FLAEKF the LQG dynamic regulator control law is given by [3], [10].

$$\boldsymbol{\tau}_k = -\mathbf{K}\hat{\mathbf{x}}_k \tag{34}$$

where; $\mathbf{K}$ is a gain matrix determined by the algebraic Riccati equation in the derivation of a LQR based on state-space form of the rigid-link robot dynamics equations. The LQR is not included in this study but the LQ gains are computed and form a component of the LQG dynamic regulator. The LQG dynamic regulator control law is fed back to form a resultant control law given by [10].

$$\boldsymbol{\tau} = \boldsymbol{\tau}_r + \boldsymbol{\tau}_k \tag{35}$$

$$\boldsymbol{\tau} = \mathbf{J}^T(\theta)\left[\mathbf{K}_p \begin{pmatrix} e_x \\ e_y \end{pmatrix} + \mathbf{K}_d \begin{pmatrix} \dot{e}_x \\ \dot{e}_y \end{pmatrix}\right] - \mathbf{K}\hat{\mathbf{x}}_k \tag{36}$$

C. Fuzzy logic adaptive vibration suppression

The FLS shown in Fig. 5 is developed intuitively with membership functions for input and output variables shown in Figs. 3 (a) and (b). Vibration suppression is achieved by adapting the control law in (13) by a fuzzy output variable λ determined in the FLS with elastic deformation inputs δ_1 and δ_2, fed back from the flexible dynamics [2]. As the magnitude of elastic transverse deformation for each link varies positively or negatively, it complements or counters deformation of the other link. Verbal descriptors for positive (P), positive maximum (PMAX), positive medium (PM), zero (ZERO) and negative (N) are used to label the membership functions shown in Figs. 3 (a) and (b) to generate nine fuzzy rules of the form;

IF δ_1 is N AND δ_2 is P THEN λ is PMAX

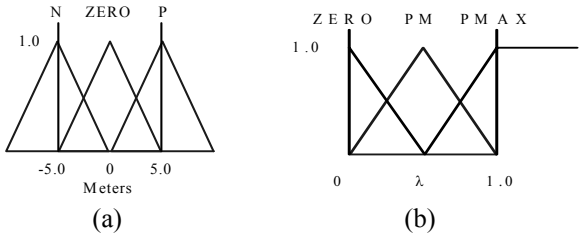

Fig. 3. Fuzzy membership functions: (a) δ_1 and δ_2, (b) Output variable λ.

The value of λ varies according to the magnitude of resultant deformation within a range from ZERO for zero deformation to PMAX for the largest deformation thereby forming a symmetric fuzzy rule matrix given in Table II. Universes of discourse range from -5 m to 5 m for δ_1 and δ_2 and 0 to 1.0 for λ. Values of δ_1 and δ_2 are normalized by gain $K_n = 5$ before entering the FLS [2].

TABLE II
FLS RULE MATRIX

		δ_2		
	λ	N	ZERO	P
δ_1	N	PMAX	PM	PMAX
	ZERO	PM	ZERO	PM
	P	PMAX	PM	PMAX

The adapted form of $\boldsymbol{\tau}_r$ in (13) is given by [2].

$$\boldsymbol{\tau}_r = K_s\lambda\left\{\mathbf{J}^T(\theta)\left[\mathbf{K}_p\begin{pmatrix}e_x\\e_y\end{pmatrix}+\mathbf{K}_d\begin{pmatrix}\dot{e}_x\\\dot{e}_y\end{pmatrix}\right]\right\} \tag{37}$$

Applying LQG dynamic regulator control in (34) to (37) provides a resultant control law given by.

$$\boldsymbol{\tau} = K_s\lambda\left\{\mathbf{J}^T(\theta)\left[\mathbf{K}_p\begin{pmatrix}e_x\\e_y\end{pmatrix}+\mathbf{K}_d\begin{pmatrix}\dot{e}_x\\\dot{e}_y\end{pmatrix}\right]\right\} - \mathbf{K}\hat{\mathbf{x}}_k \tag{38}$$

IV. SIMULATION RESULTS

Tracking without noise filtering or vibration suppression is shown in Fig, 4. Tracking with an EKF and FLAEKF shows minor improvements in Figs. 8 (a) and (b) where the FLAEKF produces a slightly better result than EKF. Tracking with FLS vibration suppression at K_s = 15 and noise filtering with EKF and FLAEKF gives nearly identical results shown in Figs. 8 (c) and (d). Tracking times are 9 min 44 sec without noise filtering or vibration suppression, 14 min 37 sec for FLS with EKF and 14 min 6 sec for FLS with FLAEKF. Matlab/Simulink™, Control Systems and Fuzzy Logic Toolboxes were used for simulation [15].

V. CONCLUSION

Vibration control of a flexible robot using an inverse dynamics strategy alone is ineffective. Minor improvements are achieved using noise filtering with FLAEKF being better than an EKF. These difficulties are overcome using FLS adaptive vibration suppression that overrides the minor effect using either an EKF or FLAEKF. The results confirm the FLS adaptive strategy is more effective in suppressing nonlinear elastic vibrations than noise filtering algorithms derived from state-space rigid-link dynamics equations.

REFERENCES

[1] A. K. Banerjee and W. Singhose, "Command shaping in tracking control of a two-link flexible robot," *AIAA Journal of Guidance, Control and Dynamics*, Engineering Note, vol. 21, no. 6, pp.1012-1015, Reston, VA, 1998.

[2] A. Green and J. Z. Sasiadek, "Adaptive control of a flexible robot using fuzzy logic," *AIAA Journal of Guidance, Control and Dynamics*, vol. 28, no. 1, pp. 36-42, AIAA, Reston, VA, 2005.

[3] A. Green and J. Z. Sasiadek "Regular and fuzzy extended Kalman filtering for a two-link flexible robot manipulator," *Proceedings of the AIAA Guidance, Navigation and Control Conference*, Reston, VA, 2001.

[4] J.Z. Sasiadek and R. Srinivasan, "Dynamic modeling and adaptive control of a single-link flexible manipulator," *Journal of Guidance, Control and Dynamics*, vol. 12, no. 6, pp. 838-844, AIAA, Reston, VA, 1989.

[5] H. Asada., and Slotine, J. –J. E., *Robot Analysis and Control*. Wiley, New York, 1986, pp. 104 -118.

[6] A.R. Fraser and R. W. Daniel, *Perturbation Techniques for Flexible Manipulators*. The Kluwer International Series in Engineering and Computer Science, vol. 138, Kluwer, Dordrecht, The Netherlands, 1991.

[7] W. T. Thomson, *Theory of Vibration with Applications*. Prentice-Hall, Upper Saddle River, NJ, 1981.

[8] De Luca, A. and B. Siciliano, "Closed-form dynamic model of planar multilink lightweight robots, *IEEE Transactions on Systems, Man and Cybernetics*, vol. 21, no. 4, pp. 826-839, 1991.

[9] W. Beres and J. Z. Sasiadek, "Finite element dynamic model of multi-link flexible manipulators," *Applied Mathematics and Computer Science,* vol. 5, no. 2, pp. 231-262, ISSI, University of Zielona Góra, Poland, 1995.

[10] F.L. Lewis, *Applied Optimal Control and Estimation-Digital design and Implementation*. Digital Signal Processing Series, Prentice Hall and Texas Instruments, 1992.

[11] R.F. Stengel, R.F. *Optimal Control and Estimation*. Dover Publications Inc., 1994.

[12] R.G. Brown and P.Y.C. Hwang, *Introduction to Random Signals and Applied Kalman Filtering*. John Wiley & Sons, 1997.

[13] J.Z. Sasiadek, J.Z. and Q. Wang, "Sensor fusion based on fuzzy Kalman filtering for autonomous robot vehicle," *Proceedings of the IEEE International Conference on Robotics and Automation*, Detroit, Michigan, May 1999.

[14] K.M. Passino and S. Yurkovich, *Fuzzy Control.* Addison-Wesley, March 1990.

[15] Matlab 6, Simulink 4, Control Systems and Fuzzy Logic Toolboxes, Release 12, The Mathworks, Inc., Natick, MA, 2001.

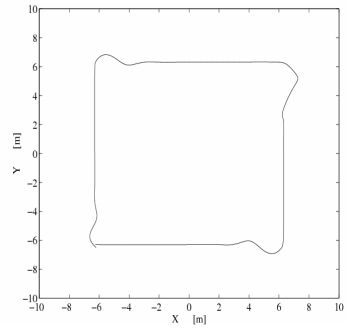

Fig. 4. Trajectory without noise filtering or vibration suppression.

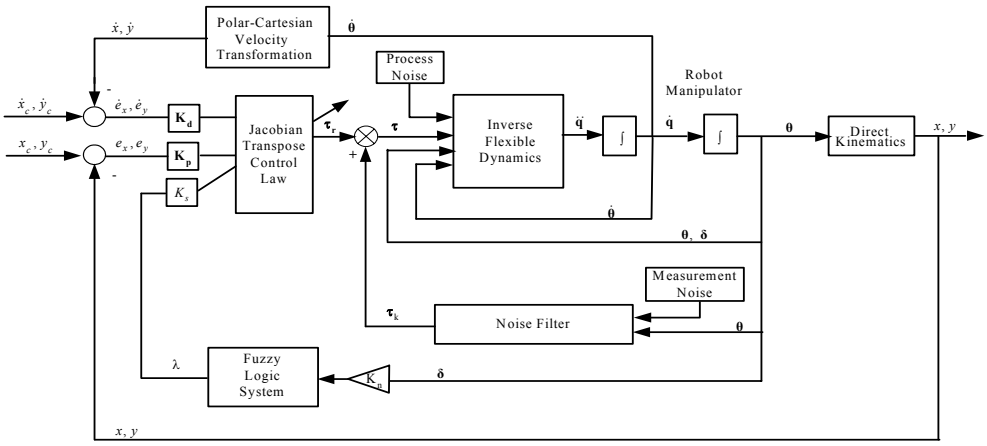

Fig. 5. Fuzzy adaptive vibration suppression and noise filtering (EKF/FLAEKF) control strategy.

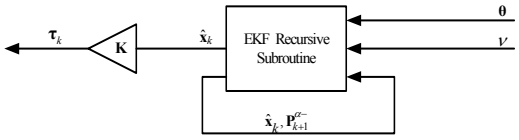

Fig. 6. LQG dynamic regulator with extended Kalman filter.

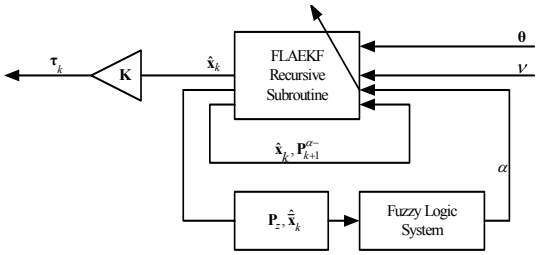

Fig. 7. LQG dynamic regulator with fuzzy logic adaptive extended Kalman filter.

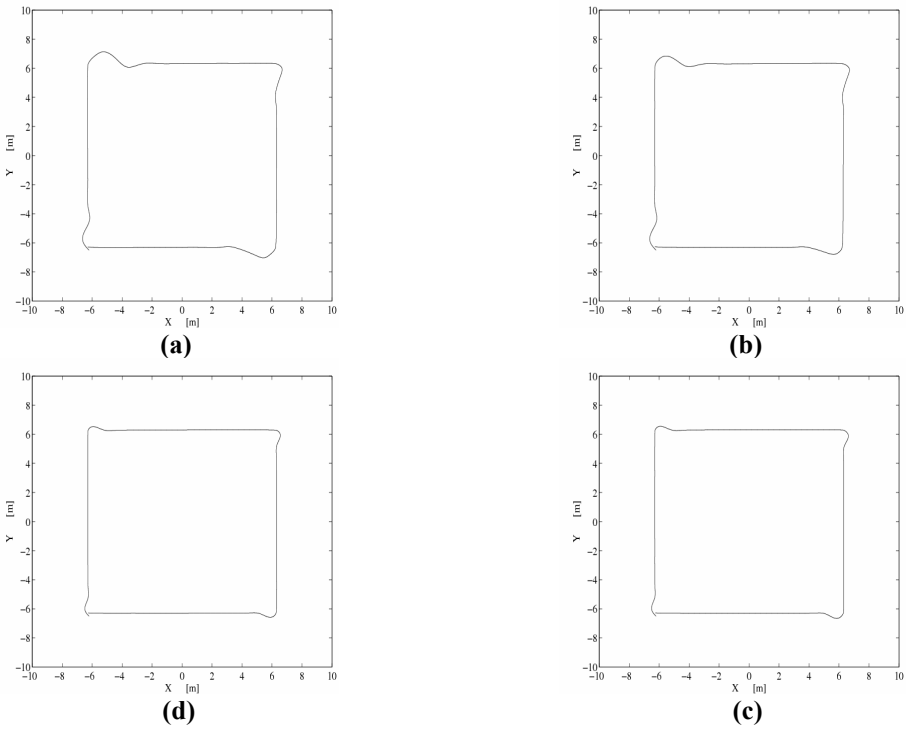

Fig. 8. Trajectories: (a) LQG dynamic regulator with EKF, (b) LQG dynamic regulator with FLAEKF, (c) FLS vibration suppression and LQG dynamic regulator with EKF, (d) FLS vibration suppression and LQG dynamic regulator with FLAEKF.